



Science Arts & Métiers (SAM)

is an open access repository that collects the work of Arts et Métiers Institute of Technology researchers and makes it freely available over the web where possible.

This is an author-deposited version published in: <https://sam.ensam.eu>
Handle ID: <http://hdl.handle.net/10985/23312>

To cite this version :

Guilherme MALACRIDA ALVES, Etienne BALMES - A time varying system perspective on rubber mount tests - In: ISMA 2022-USD 2022, Belgique, 2022-09-12 - ISMA 2022-USD 2022 (30 th International Conference on Noise and Vibration engineering) - 2022

Any correspondence concerning this service should be sent to the repository

Administrator : scienceouverte@ensam.eu



A time varying system perspective on rubber mount tests.

G. Malacrida Alves^{1,2}, Etienne Balmes^{1,2}

¹PIMM, Arts et Metiers Institute of Technology, CNRS, Cnam, HESAM Universite
151 Boulevard de l'Hôpital, 75013, Paris, France

²SDTools

44 rue Vergniaud, 75013, Paris, France

e-mail: malacrida@sdtools.com, balmes@sdtools.com

Abstract

Rubber tests typically only consider the first harmonic of responses and thus ignore additional information about variation of properties during a cycle. The Payne effect is then only described as a decrease of modulus with amplitude. An *harmonic modulation* is introduced as a novel way to look at the classical harmonic balance characterization of periodic signals in an effort to answer the question of *when in the period is the system close to being linear ?* In the case of enforced displacement tests, the harmonic modulation of force signals corresponds to an instant material stiffness or instant modulus. Sine test results are thus interpreted as trajectories in a complex modulus / strain plane that are much more discriminating than the traditional representation as a complex modulus and gives indication of coupling between hyperelastic, hysteretic and viscoelastic behaviors. This new interpretation of classical results is shown to be relevant as a correlation tool and a constitutive model for rubber is validated in its ability to reproduce the instant modulus behavior in a wide range of cases.

1 Introduction

Rubber mounts are used in many industries. In automotive applications, bushings are used to link bodies with flexibility and dissipation as well as tolerance and high strain stiffness evolution objectives. In railway applications pads control the dynamic properties of the rail/sleeper interaction. Such rubber parts exhibit hyperelastic, rate independent hysteretic behavior, as well as viscoelastic behavior as will be detailed in section 2. Discriminating between different non-linear behavior and accounting for parameter dependencies such as temperature and amplitude dependence, known as Payne effect, is a challenge and the paper will seek to extend propositions of [1, 2].

In linear system analysis the usual approach characterizes the behavior using transfer functions. For non-linear systems under harmonic loading, the usual approach is to consider multiple harmonics characterizing the non-linearity. This has in particular led to the development of the harmonic balance method and its variants [3, 4]. It is also possible to use the linear parameter varying (LPV) system [5] perspective developed by the controls community and work on instant linearization by the authors' group [6, 7]. The present work is at the cross roads between the two perspectives: one develops a strategy that considers harmonic test results but views them with a linear parameter varying understanding.

For sinusoidal excitation with an offset, or a signal only containing harmonics 1 and 0, a linear system only exhibits response at harmonic 1 and 0. Section 3 introduces *harmonic modulation* as a periodic fluctuation around the harmonic 1 and 0 trajectory. In the considered case of measured forces resulting of an enforced displacement sine test, the harmonic modulation can be interpreted as an instantaneous stiffness or modulus,

when using section properties to allow a unit change. Base behaviors are first analyzed and the constitutive model identified in [1] is used for more realistic cases.

Section 4 then addresses issues found when applying the methodology to actual test data and illustrates the usefulness of the instant stiffness signal feature in analyzing rubber tests and the Payne effect. Finally section 5 proposes a time varying application preparing for novel testing strategies.

2 A unified behavior model of rubber

Rubber models typically consider three types of behavior in hyperelasticity [8, 9], where the force only depends on position/strain but is non-linear, rate independent hysteresis, where forces depend on strain history but in a rate independent way, and viscoelasticity where loads depends on strain history but linearly and can thus be represented using a transfer function, called complex modulus in the materials community.

Figure 1, drawn from [1, 2], gives a synthetic view of typical test results which combine low constant speed ramps and sinusoidal tests at varying frequencies, amplitudes and prestress. The ramps are used to extract a base non-linear behavior shown as the red hyperelastic curve. The green dashed curves characterize the rate independent hysteresis, and the blue to yellow maps give the frequency and amplitude dependence obtained using sine tests.

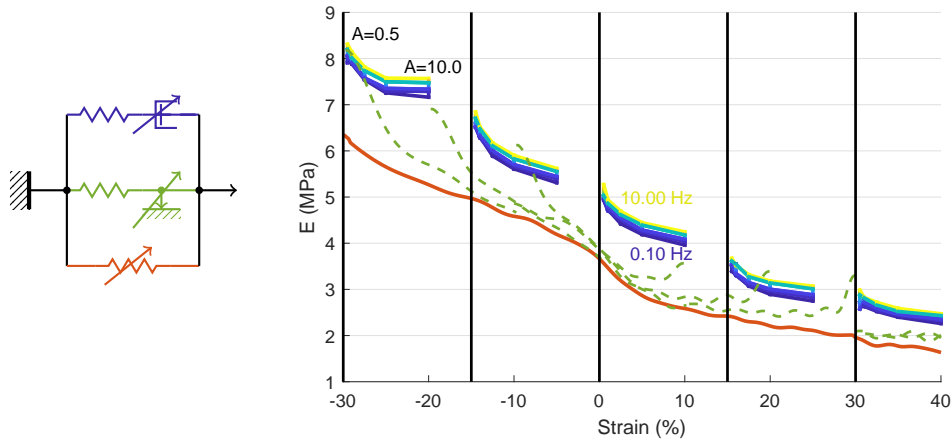


Figure 1: Unified non-parametric representation of hyperelastic (solid red), hysteretic relaxation (green, dashed), viscoelastic complex moduli (blue to yellow map).

The discussion in [1, 2] first introduces non-parametric identification phases or description of the behavior through test data. For rate independent hysteresis, the classical approach is to perform a low speed triangular test leading to an periodic response with different loading and unloading trajectories and thus a dissipated energy per cycle. The classical approximation of this curve through a discretization strategy is to consider a series of Jenkins cells and possibly an infinite series in a STS model [10]. Figure 2 illustrates two different discretizations with 3 and 5 cells. Starting from a turning point, the tangent stiffness begins at a high asymptote $\sum_{i=0}^{N_{cell}} K^i$ and tends to the lower limit K^0 . Assuming the Jenkins cells to be ordered by increasing saturation forces, the hysteretic relaxation stiffness for k sliding cells is

$$K_b^k = \sum_{i \leq k} K^i \quad (1)$$

with stiffness changes occurring at break points given by

$$x_f^i - x_{turn} = \frac{F_f^i}{K^i} \quad (2)$$

which can be used to build a relaxation modulus where force is obtained as a convolution using distance to the last turning point.

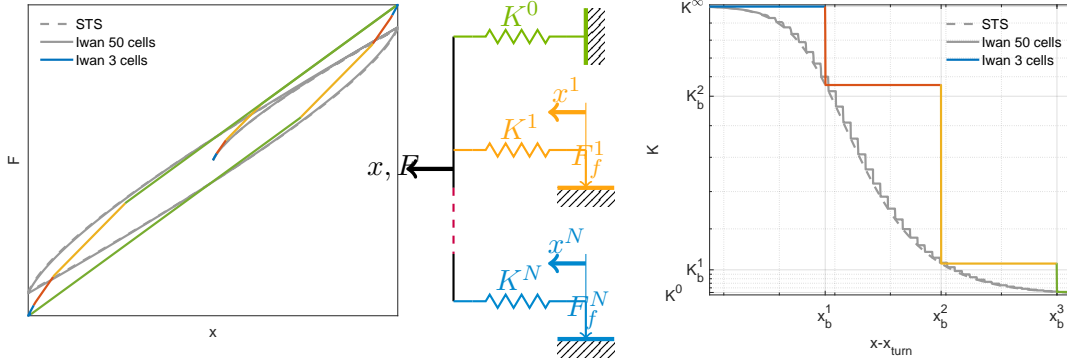


Figure 2: Scheme for Iwan model and respective response in terms of hysteretic relaxation and on force/displacement domain.

Linear viscoelasticity makes the assumption that stress depends on the history of deformation. If this dependence is linear, one can use convolution with a relaxation function in the time domain or product with a complex modulus in the frequency domain. Classical discretization approaches are rational fractions called generalized Maxwell models in the material community, or compact parametric forms such as fractional derivatives which can be approached with a controlled degree of accuracy by Maxwell models and should thus be considered as fundamentally identical model forms. For non-linear coupling, it was shown in [1, 2] that the most appropriate form considers linear relaxation of stress rate

$$\dot{F}^i + \omega^i F^i = g^i \dot{F}^{\infty}(x). \quad (3)$$

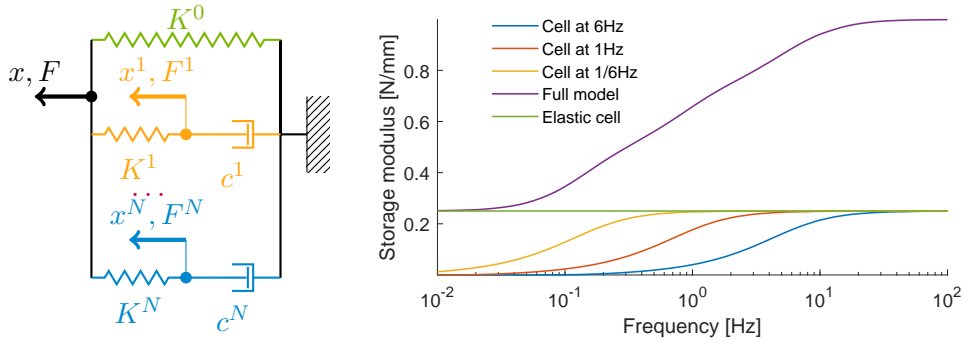


Figure 3: Generalized Maxwell model and associated frequency domain response.

Eventually, to properly represent the Payne effect it was proposed to use the non-linear viscoelasticity proposed in [11] but replacing the initial parametrization by the use of the physically meaningful saturation distance x_f^i

$$\dot{F}^i + \left(\omega^i + \frac{\|\dot{x}\|}{x_f^i} \right) F^i = \frac{g^i}{g^0} \dot{F}^0(x) \quad (4)$$

Non-linear coupling with hyperelasticity is obtained by relaxing $\dot{F}^0(x) = \partial F_0(x)/\partial t$. At sufficient velocities compared to the relaxation time $\|\dot{x}\|/x_f^i \gg \omega_i$, this non-linear cell has a fast relaxation (as its frequency follows $\omega^i + \frac{\|\dot{x}\|}{x_f^i}$) and thus behaves like hysteresis. At much lower velocities it has a linear viscoelastic behavior.

Overall a parametric model is described by a distribution of increasing relaxation frequencies ω^i , associated relaxation distances x_f^i and load fraction gains g^i . Cells with frequencies much below the band of interest or cycle amplitudes leading to significant speeds will behave non-linearly which is known as the Payne effect. The discretization error can be controlled by the number of terms/cells kept in the series.

This is just one of possible models of non-linear viscoelasticity. In [1, 2], the discrimination was performed using an notion of instant stiffness using a sliding window which while giving good results is not very general. The next section thus seeks proposes a more general strategy based on a specific analysis of harmonic balance results.

3 Harmonic modulation a time varying deviation from linear response

One considers the classical perspective of the harmonic balance methodology [3, 4] where the response is assumed periodic and one thus has for any quantity depending on time

$$\{q(t)\} = \sum_{h>=0} Re(\{q^h\} e^{ih\omega t}) \quad (5)$$

details on extraction of these components will be given in section 4.

Typical rubber tests are uni-axial shear or compression with a sinusoidal displacement so that one expects a scalar single harmonic $q(t) = Re(q^1 e^{i\omega t})$ displacement input and a multi-harmonic output force $F(t) = Re(\sum_h F^h e^{ih\omega t})$ which, for the constitutive law discussed in the previous section can be computed using the series on non-linear contributions (5).

The classical approach when characterizing the viscoelastic behavior is to ignore higher harmonics and thus use a complex stiffness/modulus [12] given by

$$[K^1] = \frac{F^1}{q^1} = [K^1]' (1 + i\eta) \quad (6)$$

and the non-linearity is only viewed for very low frequency relaxation cells analyzed as rate independent contributions or through an amplitude dependence called Payne effect.

The novel point of view taken in this work is to seek to answer a generic question : *when in the period is the system close to being linear ?* As an indicator answering this question it is proposed to replace the initial instant stiffness indicator proposed in [1] by the instant complex stiffness defined by

$$[K(t, q^0, q^1)] = \frac{\sum_{h>=1} \{F^h\} e^{i(h-1)\omega t}}{q^1}. \quad (7)$$

It is quite obvious that this indicator is constant for a linear system and the instant stiffness is then equal to the complex modulus (6). The instant stiffness (7) is also clearly periodic, with mean K^1 , thus providing indications that characterize non-linearity within the period and a clear definition of *weakly non-linear* as the case where the time dependence is small compared to the mean.

Pre-load, which is known to affect the properties of rubber materials, is fully contained in the static contribution or harmonic 0, it is thus expected that the indicator will depend on q^0 . Similarly, the Payne effect, visible as an amplitude dependence for the complex modulus maps of figure 1, indicates that a dependence of $K(t)$ on q^1 is expected.

As an illustration, one considers an hyperelastic model, interpolated using piecewise cubic polynomials, with a series of 6 branches. As a starting point, the first three associated with slow relaxation times are supposed purely hysteretic/friction branches and the last 3 viscoelastic.

In the time response over a period, the hysteretic/friction branches F_2 and F_3 show a linear response close to the turning points at $TR = 0$ and $TR = 2$ followed by a saturated load. The viscoelastic branches F_4 , F_5 show an expected sinusoidal shape. The classical polar representation of stress as a function of strain shows a parallelogram for friction and an ellipse for viscoelastic behavior.

The tangent stiffness $\partial F^i / \partial x$ shown at bottom left is difficult to exploit. In the hysteretic behavior the slope is zero for much of the cycle. In the viscoelastic behavior, the phase lag associated with dissipation generates infinite slopes at the strain maxima. The fact that the slope is not constant for hysteretic cells illustrates the use of \dot{F}^0 in defining the hysteresis.

The instant stiffness (7), shown bottom right, illustrates how the linearity of viscoelastic cells is immediately visible as the fact that the instant stiffness is constant. By zooming significantly it appears that it is not perfectly constant which comes from the use of hyperelastic load rate \dot{F}^0 in (5).

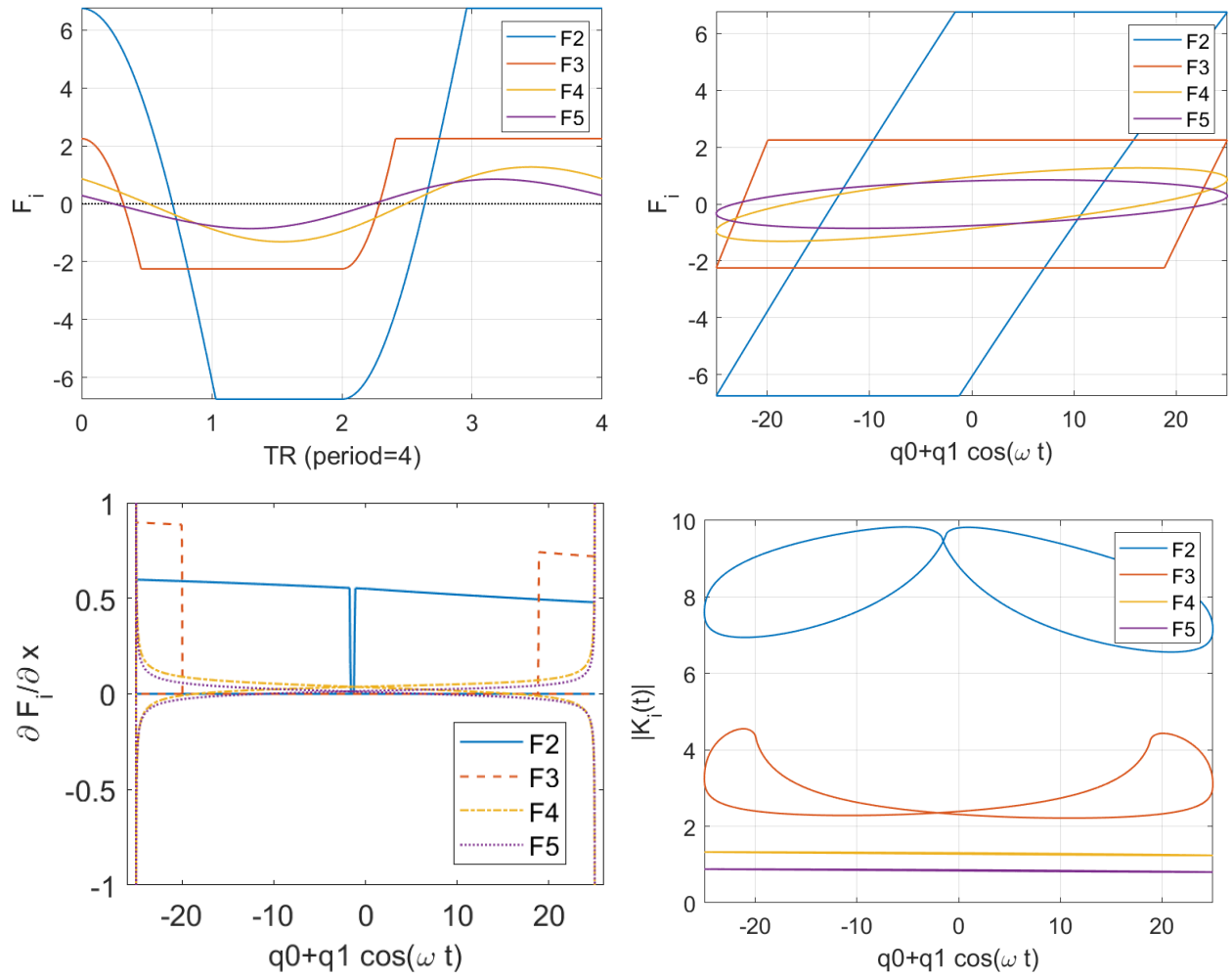


Figure 4: Top left : load in behavior branches, top right : load/strain trajectories. Bottom left : tangent stiffness, bottom right : instant stiffness from harmonic modulation

One now seeks to analyze the complete model used in [1] with 6 branches of the form (5). In figure 5 left, when comparing the time response $q(t)$ with the first harmonic $Re(q^0 + q^1 e^{i\omega t})$, shown in red, a slight deviation from sinusoidal behavior is visible but difficult to quantify. By using the *harmonic modulation* defined by

$$[q^a(t)] = \sum_{h \geq 1} \{q^h\} e^{i(h-1)\omega t} \quad (8)$$

one sees in the right plot that the amplitude of $q^a(t)$ has a 15 % deviation around the mean given by q^1 which is a constant for a purely periodic system and will be considered slowly time varying later on.

The instant stiffness phase δ it typically interpreted as a loss factor $\eta = \tan(\delta)$. The phase deviation is also a clear indication of asymmetry of the loading and unloading phases. When instant force/stiffness is increasing the harmonic modulation phase is below that of harmonic 1. The fact strain energy increases faster than expected can be interpreted as a smaller loss factor. On the contrary when the strain energy decreases faster than what the linear model would say, energy is lost which is seen as a higher than average loss factor.

Figure 5 right shows their respective harmonic modulation, as the harmonics zero and one become a constant value it becomes even more clear how the amplitude and phase oscillate around it.

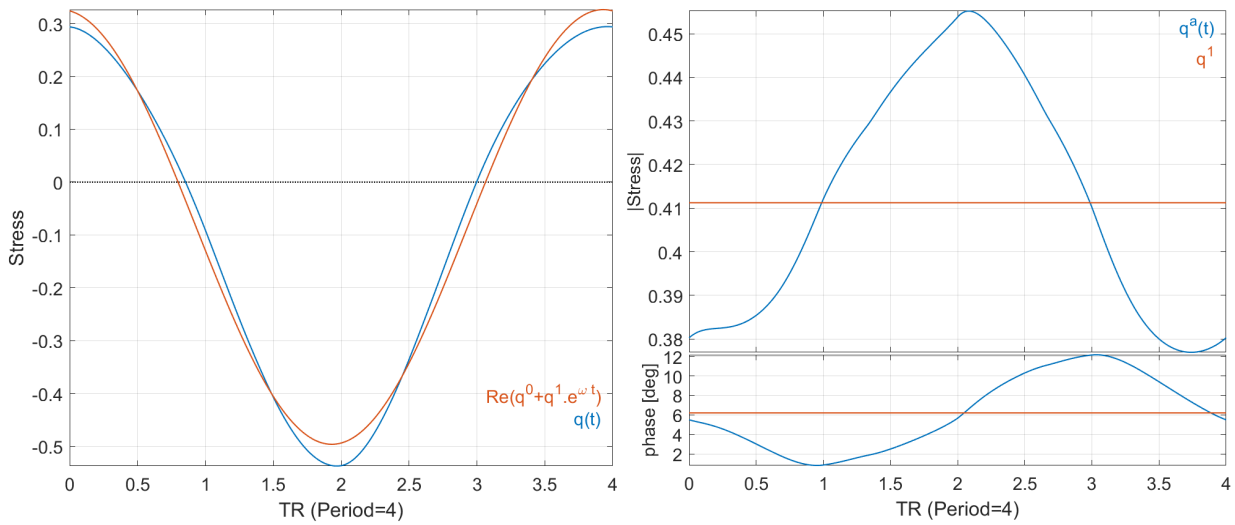


Figure 5: Left : force as function of reduced time ($1=1/4$ period). Right : harmonic modulation ($q^a(t)$ blue) and first harmonic (q^1 red).

In figure 6 left, the classical force displacement response is shown. The hyperelastic behavior is visible as global slope changes and the Payne effect in the fact that the slope of small cycles is higher than that of large cycles.

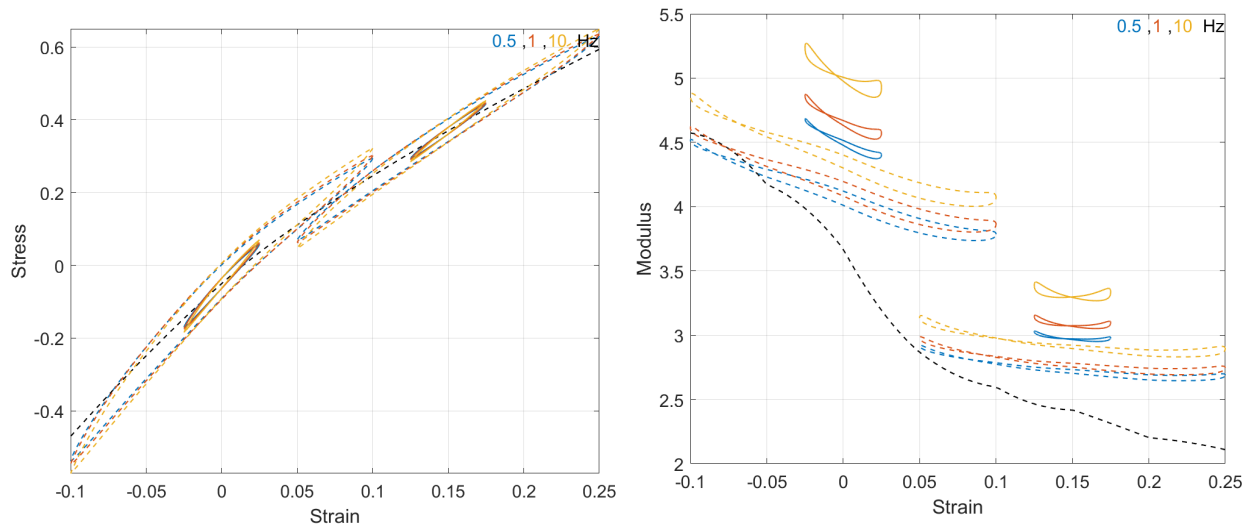


Figure 6: Left : force (or stress MPa) / displacement curve with two levels of pre-stress, two amplitudes and 3 frequencies. Right : instant stiffness (7) (or Modulus using section information). Hyperelastic force/tangent stiffness is shown as a black dotted line.

Figure 6 right illustrates how the instant stiffness is much more readable than the force displacement curves. The evolution with frequency is readily seen as an increase of modulus with frequency (as expected from figure 3). The coupling with hyperelasticity is also visible as the fact that the overall instant stiffness trajectories are not flat. Analysis of simple non-linear cases such as the Duffing oscillator can be used to show that the slope of the instant stiffness trajectory is expected to be lower than the global hyperelastic curve. For example at 0.5 Hz and strain = -0.1 the instant stiffness is below the hyperelastic curve.

The Payne effect also clearly appears as the fact that for higher amplitudes the instant stiffness is lower at all instants of the period. This corresponds to the fact that for large amplitudes low frequency relaxation cells reach saturation and thus have a decreased amplitude (see green curves in figure 1). At the center of the period, the stiffness is however still higher than the hyperelastic stiffness shown in black. This is consistent with the choice of adding non-linear viscoelastic cells to a base hyperelastic behavior.

4 Harmonic modulation from test data

In order to evaluate the applicability of the proposed instant stiffness estimation, the method was applied using sine test data from [1]. When seeking to estimate harmonics, the first obvious choice is to use FFT. From a 10 period signal, figure 7 illustrates the results for excitation at 0.5 Hz, zero average strain and two strain amplitudes: 2.5% and 10%. On the left, the stress spectrum shows a noise floor around 10^{-4} MPa for both cases. For the low amplitude test (blue) only the first and second harmonics are visible, while on the high amplitude (red) up to 6 harmonics can be seen. Figure 7 right shows two estimations of the instantaneous stiffness. For black dots build the harmonic modulations by a left shift of the spectrum keeping the noise and all harmonics. The results are clearly very noisy. A much more consistent result, shown in colored bold lines, is obtained using only the first 7 harmonics.

As side issues visible in figure 7, one can note a small leakage issue which may be due to frequency or amplitude modulation. One can also view that the instant stiffness phase or rather its tangent the instant loss factor, shown as color, has the expected variations discussed in the previous section.

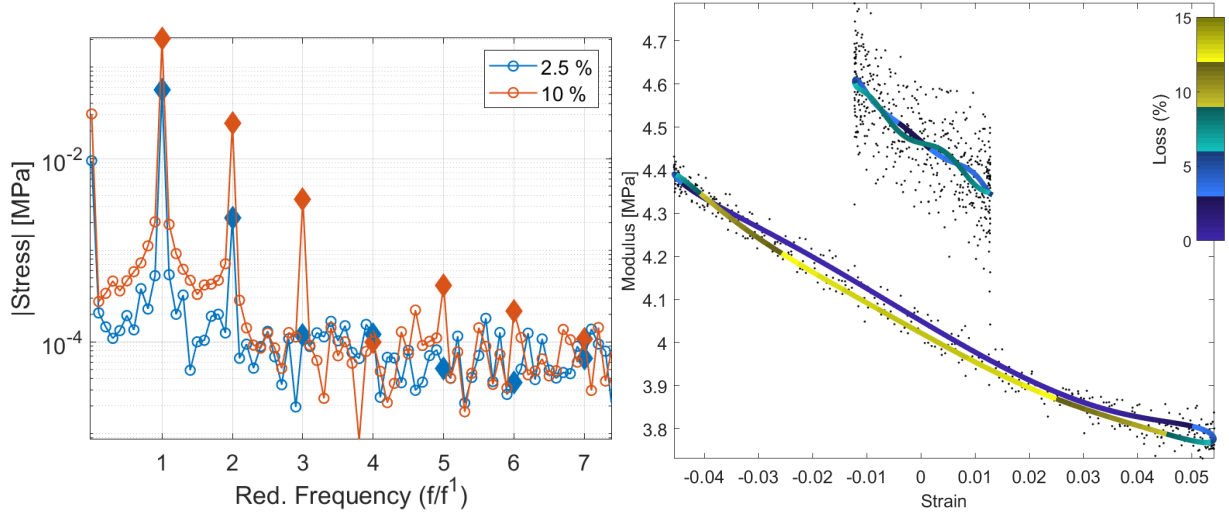


Figure 7: Enforced strain tests (10 cycles) at 0.5 Hz. Left : Stress spectrum for two different excitation levels with harmonics of the excitation frequency highlighted Right : Respective instantaneous stiffness estimation with a complete signal (dotted) and only harmonics up to seven (bold) in function of strain

In the long term, best accuracy in the presence of noise will be achieved using a signal model. For example, [13] uses a signal model where an harmonic component is described by three state variables: a real part, an imaginary part, and an instantaneous frequency. This opens the possibility to estimate the signal state vector using an extended Kalman filter (EKF), which handles noise, tracks slow signal variations, and allows the a priori selection of retained harmonics.

While the estimation using the algorithms in [13] were successful in other applications with cleaner data, the results were actually poor for the present case. The proposed strategy is thus to use a state vector of the form

$$\{x(t)\} = \{q^0(t) \quad \dots \quad q^h(t) \quad \dots \quad \omega(t) \quad \phi_R(t)\}^T \quad (9)$$

that considers only the q^h coefficient tied to each harmonic, the current frequency ω and the phase associated with harmonic 1 of a reference signal $\phi_R(t)$. In a discrete time description the evolution of $\phi_R(t)$ is approximated, in an explicit scheme, by an evolution equation.

$$\phi_R^{t+1} = \phi_R^t + dt\omega^t \quad (10)$$

All other states are expected to be perfectly constant for a time invariant non-linear system under periodic excitation and varying slowly in time with frequencies much below ω for the case of interest. The original signal can be recovered via an observation equation

$$y(t) = \sum_{h=0}^{h_{max}} [\cos(h\phi) \quad -\sin(h\phi)] \begin{Bmatrix} Re(q^h(t)) \\ Im(q^h(t)) \end{Bmatrix} + e(t) \quad (11)$$

where $e(t)$ is assumed to be a noise not correlated with harmonics. As our implementation of the EKF strategy is not yet robust enough, the results of the next section are obtained using an FFT with a sliding window of 1 period.

Section 5 will discuss how instantaneous estimations could be applied to slowly varying conditions, an amplitude sweep for example.

5 Time varying test scenario

The end objective of this work is to generalize characterization of non-linear coupling. As an illustration of possibilities one considers and experiment where for a constant frequency of 10 Hz, one performs two amplitude sweeps from 0.05% strain to 0.15%. As this is not a standard test, the interest is analyzed using the non-linear model identified in [1].

The trajectories in the stress/strain plane in figure 8 left, and even more convincingly in the instant modulus/strain plane in figure 8 right, illustrate the features to be reproduced in an accurate constitutive model

- the classical complex modulus which corresponds to the global level given by harmonic 1
- the trajectory in the strain/modulus plan: harmonic 2 gives the overall slope, harmonic 3 gives a curvature, ...
- the loss/phase at instants of the trajectory : harmonic 2 generates loss decrease for increasing stiffness, ...
- to ease interpretation and accurate constitutive law identification, it would certainly help to extract curves giving instant modulus and loss factor as a function of strain phase, cycle amplitude, excitation frequency, ...

The harmonic modulation used here gives much better results than the previous definition used in [1]. The overall shape and phase changes of figure 7 right and 8 right are quite similar (note that the overall level is expected to be different since two distinct frequencies are used) and clearly confirm the choice of . The fact that alternatives to (5) give much poorer match will be shown in the presentation.

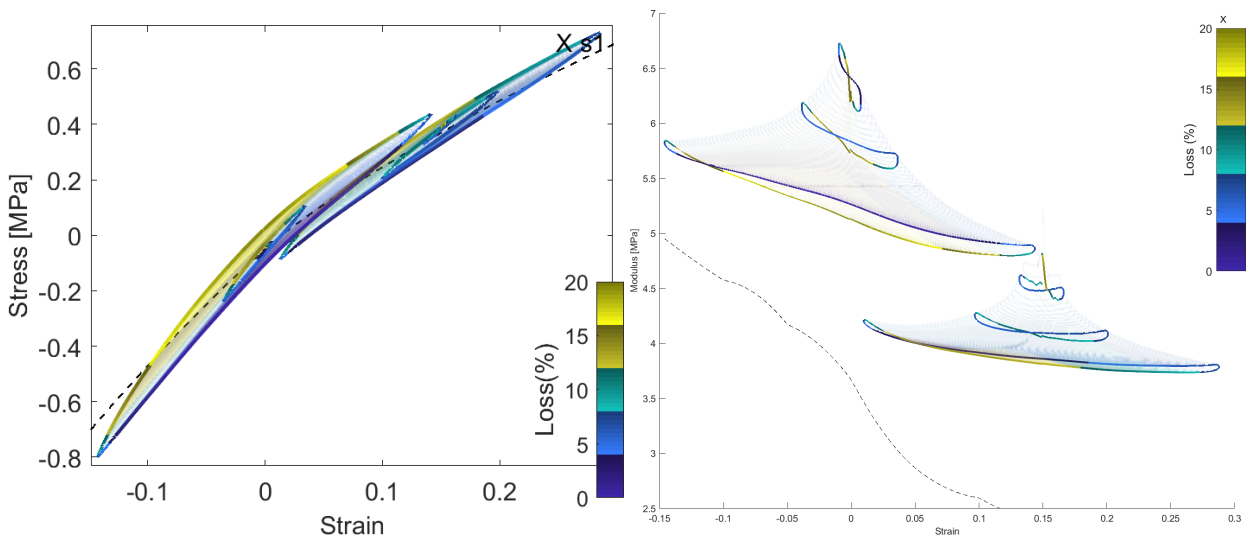


Figure 8: Amplitude sweeps at 10 Hz and two pre-stress levels. Left: stress as function of strain, right instant modulus as function of strain. Color : instant loss factor

It is interesting to note a few features that should be checked against actual tests. For 15% pre-strain and large amplitudes the loss varies less than for 0% pre-strain. This is expected since the modulus variation smaller, but one should see how if this gives results consistent with (5). The first period at 15% pre-strain has an obvious stabilization problem. This effect is certainly enhanced by the use of a sliding FFT rather than a signal model estimate and should be corrected.

6 Conclusion

Classical rubber tests typically only consider the first harmonic of tests and thus ignore additional information about variation of properties during a cycle. The Payne effect is thus only described as a decrease of modulus with amplitude. The *harmonic modulation* was introduced as a novel way to look at the classical harmonic balance characterization of periodic signals and seek to answer the question of *when in the period is the system close to being linear ?* In the case of enforced displacement tests, the harmonic modulation of force signals corresponds to an instant material stiffness or instant modulus. Sine test results are thus interpreted as trajectories in a complex modulus / strain plane that are much more discriminating than the traditional representation and gives indication of coupling of hyperelastic, hysteretic and viscoelastic behaviors.

This new interpretation of classical results was shown to be relevant as correlation tool and the proposed constitutive model for rubber is thus validated in its ability to reproduce the instant modulus behavior in a wide range of cases. Extensions of the base idea are to use a harmonic signal model to analyze responses of systems that are slowly time varying. This was used to illustrate the interest of amplitude sweeps for improved material characterization, but the end objective of this project is to analyze brake squeal limit cycles [14].

Acknowledgements

The thesis of the first author is funded by a CIFRE convention with ANRT and a project with Hitachi Astemo, Brake Business, Drancy. The test were performed by Vibracoustic.

References

- [1] R. Penas, E. Balmes, A. Gaudin, *A unified non-linear system model view of hyperelasticity, viscoelasticity and hysteresis exhibited by rubber*, MSSP, Vol. 170, (2022), pp. 25.
- [2] R. Penas, *Models of dissipative bushings in multibody dynamics*, Ph.D. thesis, Ecole Nationale Supérieure d'Arts et Métiers Paris (2021).
- [3] V. Jaumouillé, J.-J. Sinou, B. Petitjean, *An adaptive harmonic balance method for predicting the non-linear dynamic responses of mechanical systems. Application to bolted structures*, Journal of Sound and Vibration, Vol. 329, (2010), pp. 4048–4067.
- [4] J. J. Sinou, *Dynamique Non-Linéaire Des Structures Complexes, Fixes et Tournantes. Approches Théoriques, Numériques et Expérimentales.*, Ecole Centrale de Lyon, Université Claude Bernard (2008).
- [5] M. Gilson, V. Laurain, R. Tóth, H. Garnier, *Direct identification of continuous-time linear parameter-varying input/output models*, IET Control Theory & Applications, Vol. 5, No. 7, (2011), pp. 878–888.
- [6] G. Vermot Des Roches, *Frequency and time simulation of squeal instabilities. Application to the design of industrial automotive brakes*, Ph.D. thesis, Ecole Centrale Paris, CIFRE SDTools (2011).
- [7] G. Vermot Des Roches, E. Balmes, *Understanding friction induced damping in bolted assemblies through explicit transient simulation*, ISMA, KUL, ID360.
- [8] T. Beda, *Modeling hyperelastic behavior of rubber: A novel invariant-based and a review of constitutive models*, Journal of Polymer Science Part B: Polymer Physics, Vol. 45, No. 13, (2007), pp. 1713–1732.

- [9] G. Marckmann, E. Verron, *Comparison of hyperelastic models for rubber-like materials*, Rubber Chemistry and Technology, Vol. 79, No. 5, (2006), pp. 835–858.
- [10] B. Bourgeteau, *Modélisation numérique des articulations en caoutchouc de la liaison au sol automobile en simulation multi-corps transitoire*, Ph.D. thesis, Ecole Centrale Paris (2009).
- [11] P. Höfer, A. Lion, *Modelling of frequency- and amplitude-dependent material properties of filler-reinforced rubber*, Journal of the Mechanics and Physics of Solids, Vol. 57, No. 3, (2009), pp. 500–520.
- [12] American Society for Testing and Materials, *ASTM E756-98 : Standard Test Method for Measuring Vibration-Damping Properties of Materials*, Annual Book of Standards, Vol. 14.02, ASTM International (1998).
- [13] J.-L. Dion, C. Stephan, G. Chevallier, H. Festjens, *Tracking and removing modulated sinusoidal components: A solution based on the kurtosis and the Extended Kalman Filter*, Mechanical Systems and Signal Processing, Vol. 38, No. 2, (2013), pp. 428–439.
- [14] G. Martin, E. Balmes, G. Vermot Des Roches, T. Chancelier, *Squeal measurement with 3D Scanning Laser Doppler Vibrometer: Handling of the time varying system behavior and analysis improvement using FEM expansion*, ISMA, KUL.